High order normal form construction near the elliptic orbit of the Sitnikov problem

Article *in* Celestial Mechanics and Dynamical Astronomy · December 2011

DOI: 10.1007/s10569-011-9380-0

2 authors:

Sara Di Ruzza
Università degli Studi di Palermo

Christoph Lhotka
University of Rome Tor Vergata

Celest Mech Dyn Astr (2011) 111:449–464
DOI 10.1007/s10569-011-9380-0

ORIGINAL ARTICLE

High order normal form construction near the elliptic orbit of the Sitnikov problem

Sara Di Ruzza · Christoph Lhotka

Received: 20 July 2010 / Revised: 18 July 2011 / Accepted: 3 September 2011 /
Published online: 22 September 2011

Abstract We consider the Sitnikov problem; from the equations of motion we derive the approximate Hamiltonian flow. Then, we introduce suitable action–angle variables in order to construct a high order normal form of the Hamiltonian. We introduce Birkhoff Cartesian coordinates near the elliptic orbit and we analyze the behavior of the remainder of the normal form. Finally, we derive a kind of local stability estimate in the vicinity of the periodic orbit for exponentially long times using the normal form up to 40th order in Cartesian coordinates.

Keywords Sitnikov problem · Normal form · Birkhoff coordinates · Exponential stability · Perturbation theory · Lie–series expansions

1 Introduction

The Sitnikov problem is a subsystem of the restricted 3–body problem with a special geometrical configuration: two equal mass bodies $m_1 = m_2$, called primaries, are moving on Keplerian orbits in an invariant plane (x, y) around their common barycenter; a third massless body m is constraint to move along the z-axis only ($x = y = 0$), (see Fig. 1). The Hamiltonian describing the motion of the third body is derived from the general Newtonian gravitational 3–body problem by setting the gravitational constant G, the unit distance $2a = a_1 + a_2$ (where a_1, a_2 are the semi–major axes of the primaries) as well as the total mass of the system $m_1 + m_2$ to unity and by setting $m = 0$. In these units, one revolution period of the primaries around the common center of gravity is $T = 2\pi$. In this setting the Hamiltonian reads:

S. Di Ruzza (✉) · C. Lhotka
Dipartimento di Matematica, Università di Roma Tor Vergata,
Via della Ricerca Scientifica 1, 00133 Roma, Italy
e-mail: saradiruzza@gmail.com

C. Lhotka
e-mail: lhotka@mat.uniroma2.it

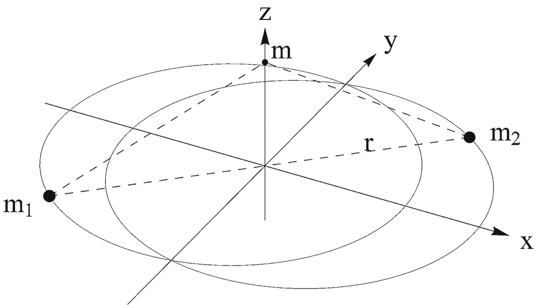

Fig. 1 A massless body m is moving along the z-axis in the time–dependent gravitational field of two primaries m_1 and m_2

$$H(z, v_z, t) = \frac{{v_z}^2}{2} - \frac{1}{\sqrt{z^2 + r(t)^2}}, \tag{1}$$

where $v_z = \dot{z}$ is the velocity of the third body and $r(t)$ is the distance between the primaries and the center of gravity; we note that $r(t)$ is a known function of the time and of the eccentricity of the Keplerian orbits of the primaries.

The system was introduced by Sitnikov to show the existence of oscillatory motion in the 3–body problem (Sitnikov 1960). It can be seen as a generalization of simpler problems, on the one hand the MacMillan problem (MacMillan 1913), in which the distance of the primaries from the center of gravity is assumed to be constant (circular motion of the primary bodies) and on the other hand the 2–center problem, in which the positions of the primaries are kept constant but the third body is allowed to move arbitrarily in space.

Due to the time dependence, the dynamical system (1) is not integrable and allows the analysis of the complete zoo of complex motions (quasi–periodic, oscillatory and chaotic) found in Celestial Mechanics.

After Sitnikov introduced the problem to answer important questions of the mid of last century, the problem was further analyzed in great detail in Moser's book on "Stable and Random Motions in Dynamical Systems" (Moser 1973). In the upcoming years the scientific community found its interest in it again; the system served as a basic model to test and validate new perturbative techniques and to show the chaotic nature of dynamical systems in its full nature.

In 1990, Liu and Sun investigated the problem by means of an analytically derived conformal mapping. In 1992, Hagel , using perturbation theory, obtained a solution of the linearized and nonlinear equation and in the same year, Hagel and Trenkler (1993) used a technique to find approximate integrals of motion for high eccentricity values of the primaries, but only for small oscillations. In 1993, Dvorak using numerical integrations showed that invariant curves exist for small oscillations centering on the barycenter. In 2003, Faruque provided analytical approximations to the MacMillan and Sitnikov problem. In 2005, Hagel and Lhotka derived analytical approximated solutions to the elliptic problem, using Floquet and Courant–Snyder theories.

The problem was also extended by considering the third body with a non–negligible mass (*extended Sitnikov problem*) by Dvorak and Sun in 1997 and in 2007 by Soulis, Bountis, Dvorak , who considered also the case in which the third body could move off the z-axis (*generalized extended Sitnikov problem*). In 2009, Hagel derived an analytical expression for the perihelion motion of the primaries, when the third body has a finite mass; in the same year, Bountis and Papadakis (2009) analyzed the problem in great detail for an arbitrary number of primary masses; Kovács and Érdi (2009) investigated special kinds of chaotic motions in the problem. Quite recently, Sidorenko (2011) complemented the previous work on the alternation of stability and instability in the family of vertical motions.

The present paper is concerned with the implementation of a numerical construction of high order normal form near elliptic equilibria. The aim of this article is to write a suitable normal form of the Hamiltonian describing the Sitnikov model near its periodic orbit. Then, the remainder of the normal form is used in order to find an exponential stability.

The paper is organized as follows: the next Section defines the formalism used throughout this paper. It states the equations of motion of the problem of interest and derives the approximate Hamiltonian flow on which the subsequent analysis is based. Via a canonical transformation into action–angle variables, the system is transformed into a suitable form for canonical perturbation theory. In the next step, we derive in Sect. 3 the high order normal form of the Sitnikov's Hamilton function. For this reason, we implement a normal form algorithm with exact coefficients to derive the normalized frequency up to the optimal order of truncation for larger values of the small parameters and extend our results by a normal form algorithm, written in Fortran, maintained by Efthymiopoulos, based on Lie–series expansions. The former was used to explicitly construct the normal form to low orders maintaining the dependence of the Fourier series on the small parameters and used for the ongoing transformations. The latter was used to find numerically the remainder function of the normal form also at higher orders (40th). Then, due to the singularity of the action–angle variables near the elliptic equilibrium (see Fassò et al. 1998, Guzzo et al. 1998), in Sect. 4, we perform a suitable transformation introducing Cartesian coordinates in order to analyze the behavior of the Hamiltonian near the elliptic equilibrium. Through the analysis of the behavior of the remainder of the normal form and through the study of the generating function we provide some stability results.

The problem is particularly interesting because at the present stage, the analyzed problem is not covered by a theorem. In fact, there are no Nekhoroshev-like theorems (see Nekhoroshev 1977) that can be applied to our model due to the singularity of the action–angle variables and due to the fact that the Hamiltonian is non isochronous. We want to underline that in this article we derive the first construction of high order normal forms around periodic orbits with the correct use of Cartesian coordinates for stability estimates.

2 Formalism and equations of motion

The equations of motion for the massless body can be derived from (1), by setting $\dot{z} = v_z$ and $\dot{v_z} = -\partial H/\partial z$:

$$\ddot{z} = -\frac{z}{\left(z^2 + r(t)^2\right)^{3/2}}, \tag{2}$$

which serves as the basic equation for the numerical results in this paper. For the analytical theories, we limit our interest to the region close to the barycenter; we therefore expand the fractional part of Eq. (2) into Taylor series as:

$$\ddot{z} = -\sum_{k=0}^{\infty} \binom{-\frac{3}{2}}{k} \frac{z^{2k+1}}{r(t)^{2k+3}}, \tag{3}$$

where the brackets stand for binomial coefficients and the convergence of the series is fulfilled assuming $|z(t)/r(t)| < 1$. We are left to express the distance r of the Keplerian problem in terms of the semi–major axis a, the eccentricity e and the mean anomaly M (see Stumpff 1959):

$$r(t) = a\left(1 + \frac{e^2}{2} - 2e\sum_{\gamma=1}^{\infty}\frac{\partial J_\gamma(\gamma e)}{\partial e}\frac{\cos(\gamma t)}{\gamma^2}\right). \tag{4}$$

Here J_γ are Bessel functions of the 1st kind. For the sake of simplicity we choose $M = t$, which is true if we set $t_0 = 0$. In this setting the initial position of the primaries is at their pericenters, since $M = nt + t_0$ and $n = 1$ in our present units. Note that, since we set $2a = a_1 + a_2 = 1$, it also follows that $a = 1/2$. Inserting (4) into (3) and expanding to a finite order in z and e, we get the equation of motion in Poisson–series–like form:

$$\ddot{z} = 8z + \sum_{\beta=0}^{N}\sum_{\alpha=0}^{\beta}\left(c_{\alpha,\beta-\alpha}e^\alpha z^{\beta-\alpha}\cos(k_{\alpha,\beta}t) + d_{\alpha,\beta}e^\alpha z^{\beta-\alpha}\right), \tag{5}$$

where $c_{m,n}$, $d_{m,n}$ are real and $k_{m,n}$ are integer numbers (m, n being indices). The integer N labels the expansion order. Note that, due to the presence of $d_{m,n}$, the disturbing part (the double sum) also consists of non–zero average terms.

For the integrable approximation $e = 0$ and small oscillations $|z| << 1$ the approximate equation of motion (5) turns out to be the one of the harmonic oscillator with natural frequency $\omega_0 = \sqrt{8}$. Within these assumptions, the massless body performs small oscillations with period ω_0 around the equilibrium configuration. In the perturbed case however, the invariant curves around the origin are slightly deformed or break up into higher order resonant islands. The generic behavior is shown with a Poincaré (or stroboscopic) map in Fig. 2. The numerical obtained phase portrait (using the map condition $r(t) = r_{\min}$) for eccentricities of the primaries $e = 0.1$ shows an equilibrium point[1] at the origin surrounded by invariant curves of harmonic oscillator type with frequency close to ω_0. Increasing the distance from the center, resonant islands show up, themselves surrounded by invariant curves. Close to the separatrices, separating the higher order resonant islands from the main island, chaos is present. The outer white regions label escape orbits going away from the system within a small number of revolution periods of the orbits, while oscillatory type orbits lie within the chaotic sea and may extend to $z \to \pm\infty$.

To understand the nonlinear (and time dependent) effects close to the center, we perform a canonical transformation to action–angle variables of the harmonic oscillator[2] by setting:

$$\begin{aligned} z &= \sqrt{\omega_0^{-1}2J_1}\sin\phi_1, \\ v_z &= \sqrt{\omega_0 2J_1}\cos\phi_1. \end{aligned} \tag{6}$$

Then we extend the phase space by setting $\phi_2 \equiv t$ and introducing the conjugated variable $T = J_2$. The use of series expansions of the form (3) and (4) together with (6) will transform the system (1) into a suitable form to implement canonical perturbation theories, as

$$H' = \omega_0 J_1 + J_2 + \sum_{k=1}^{N}\omega_k(J_1; e) + \sum_{(k,l)\in\mathbb{Z}^2} p_{k,l}(J_1; e)\cdot\cos(k\phi_1 + l\phi_2) \tag{7}$$

where ω_k and $p_{k,l}$ are polynomials in J_1 and e. Note that the perturbation of the unperturbed problem is again split into non–zero and zero average contributions, like in the formulation

[1] Note that, due to the periodic time dependence of the Hamiltonian, the origin is a periodic orbit in the extended phase space.

[2] Note that the choice of the action–angle variables of the harmonic oscillator is valid only within the present simplifications. It is well known (see Belbruno et al. 1994), that the solution of the integrable approximation can be expressed in terms of elliptic functions.

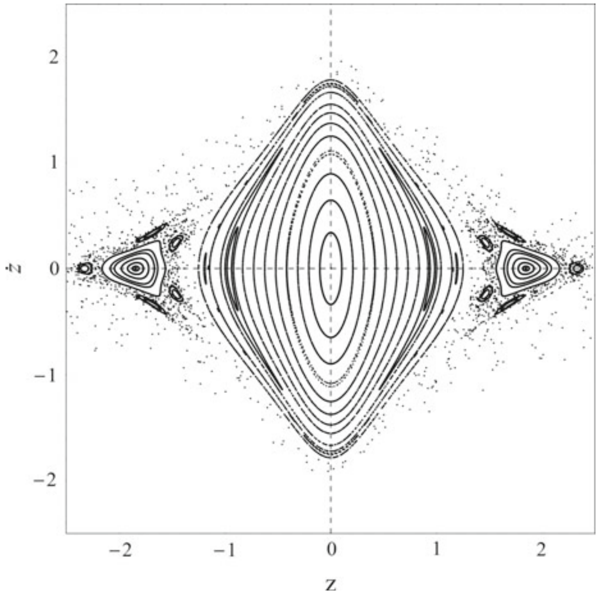

Fig. 2 Poincaré map obtained from Eq. (2) for $e = 0.1$. Our region of interest for the analytical investigations is limited to $|z(t)|/|r(t)| < 1$ (see text)

of the equation of motion (5). The frequency vector of unperturbed motion in this setting is given by $\omega = \partial H'/\partial J = (\omega_0, 1)$, where $J = (J_1, J_2)$. We note that all terms depending only on t do not contribute to the dynamics in the (z, v_z)–plane and can be ignored.

We label the summands in (7) of same order of magnitude in the monomials $e^\alpha J^\beta$ by $\lambda = \alpha + 2\beta$, such that the Hamiltonian can also be written into the simpler form:

$$
\begin{aligned}
H' &= h_0\left(J_1, J_2\right) + \sum_{\lambda=1}^{N} h_\lambda, \\
h_\lambda &= \sum_{\alpha+2\beta=\lambda} c_{\alpha,\beta} e^\alpha {J_1}^\beta \cos\left(k_{1_{\alpha,\beta}}\phi_1 + k_{2_{\alpha,\beta}}\phi_2\right),
\end{aligned}
\tag{8}
$$

for suitable $\alpha, \beta \in \mathbb{N}$, $c_{\alpha,\beta} \in \mathbb{R}$, $k_{1_{\alpha,\beta}}, k_{2_{\alpha,\beta}} \in \mathbb{Z}$. In the above setting, for $N = 4$, the Hamiltonian reads:

$$
\begin{aligned}
h_0 &= 2\sqrt{2}J_1 + J_2, \\
h_1 &= h_2 = 0, \\
h_3 &= 3\sqrt{2}eJ_1\cos\phi_2 - \frac{3eJ_1\cos\left(2\phi_1 - \phi_2\right)}{\sqrt{2}} - \frac{3eJ_1\cos\left(2\phi_1 + \phi_2\right)}{\sqrt{2}}, \\
h_4 &= \left(3J_1^2 - \frac{3e^2J_1}{\sqrt{2}}\right)\cos 2\phi_1 - \frac{9e^2J_1\cos\left(2\phi_1 - 2\phi_2\right)}{2\sqrt{2}} - \frac{9e^2J_1\cos\left(2\phi_1 + 2\phi_2\right)}{2\sqrt{2}} \\
&\quad + \frac{3e^2J_1}{\sqrt{2}} + \frac{9e^2J_1}{\sqrt{2}}\cos 2\phi_2 - \frac{3}{4}J_1^2\cos 4\phi_1 - \frac{9J_1^2}{4}.
\end{aligned}
\tag{9}
$$

3 Birkhoff normal form

In this Section we summarize the main steps to implement the normal form algorithm for nearly–integrable Hamiltonian systems of the form:

$$H = h_{int}(J) + h_\varepsilon(J, \phi)$$

where (J, ϕ) are action–angle variables of dimension d and h_{int}, h_ε are the integrable and the perturbing part, respectively. In our case, recalling (8), $h_{int} = h_0(J_1, J_2)$, $h_\varepsilon = \sum_{\lambda=1}^{N} h_\lambda$. The corresponding canonical set of equations of motion for $k = 1, \ldots, d$ ($d = 2$ in our case) is given by:

$$\begin{aligned}
\frac{d\phi_k}{dt} &= \frac{\partial H}{\partial J_k} = \omega_k(J) + \frac{\partial h_\varepsilon}{\partial J_k}(J, \phi),\\
\frac{dJ_k}{dt} &= -\frac{\partial H}{\partial \phi_k} = -\frac{\partial h_\varepsilon}{\partial \phi_k}(J, \phi), \quad k = 1, \ldots, d,
\end{aligned}$$

where $\omega(J) = (\omega_1(J), \ldots, \omega_d(J))$ defines the frequency vector of the integrable approximation of the system for vanishing perturbation parameter ($\varepsilon = 0$), which we assume far away from a resonant condition. The natural question arises, up to which threshold of the parameter ε the system behaves alike the integrable approximation of it. The idea is to find a canonical transformation $(J, \phi) \to (J', \phi')$ from old to new variables, such that the perturbing effects become minimal, in the best case negligible:

$$\begin{aligned}
\frac{d\phi'_k}{dt} &= \frac{\partial H'}{\partial J'_k} = \omega'_k(J') + O(J', \phi'),\\
\frac{dJ'_k}{dt} &= -\frac{\partial H'}{\partial \phi'_k} = O(J', \phi')
\end{aligned} \tag{10}$$

where H' is the Hamiltonian in new variables, ω' denotes the new frequency in terms of the new variables and $O(J', \phi')$ stands for higher order terms. The Eqs. (10) define the normal form of the dynamical system up to normalization order n.

The method to obtain the suitable normal form is implemented by using standard Lie–transformation theory, (see Efthymiopoulos 2008, Ferraz–Mello 2006 or Giorgilli 2002) for further details). Defining the Lie–derivative $l_W = \{\cdot, W\}$ where the curly brackets stand for the Poisson brackets, the Lie–operator L_W can be defined as the exponential of it, say $L_W = e^{l_W}$. For the full set of properties of the operator, we refer to one of the papers suggested above; for the present approach we only need two fundamental aspects of it:

i) an ε–close canonical transformation from old $(J^{(0)}, \phi^{(0)})$ to new $(J^{(1)}, \phi^{(1)})$ variables can be implemented using the Lie–operator:

$$J^{(1)} = e^{\varepsilon l_{W_1}} J^{(0)}, \quad \phi^{(1)} = e^{\varepsilon l_{W_1}} \phi^{(0)};$$

we use a fundamental result that claims the time–evolution of the action–angle variables of a Hamiltonian system $H(J, \phi)$ can be written in terms of

$$J(t) = e^{t l_H} J(0), \quad \phi(t) = e^{t l_H} \phi(0),$$

to generate a symplectic transformation in phase space, where we essentially replace the Hamiltonian through a generating function W_1 and the time flow in t through the parameter flow in ε.

ii) The Lie–operator is flat, namely we are able to replace

$$f\,(L_W J, L_W\phi) = L_W f(J,\phi),$$

leading to the effect that, under change of variables, the Hamiltonian transforms accordingly:

$$H^{(1)}\left(J^{(1)},\phi^{(1)}\right) = e^{\varepsilon l_{W_1}} H^{(0)}\left(J^{(0)},\phi^{(0)}\right).$$

Expanding the exponential and the perturbing part into Taylor–series in ε:

$$H^{(1)} = (1+\varepsilon l_{W_1}+\cdots)\,(h_0(J)+\varepsilon h_1(J,\phi)+\cdots)\,,$$

we get order by order:

$$\begin{aligned}\varepsilon^0 &: h_0,\\ \varepsilon^1 &: l_{W_1}h_0 + h_1,\end{aligned}$$

and similar for higher orders. The normal form Eqs. (10) imply that our aim is to remove the dependence on the angles. Splitting the perturbing part of first order into $h_1 = \bar{h}_1(J) + \tilde{h}_1(J,\phi)$ and implementing the Poisson brackets, we get the condition on the generating function W_1:

$$\{h_0, W_1\} + \tilde{h}_1 = 0,$$

which is called the homological equation. Assuming a Fourier expansion of $\tilde{h}_1$ of the form

$$\tilde{h}_1 = \sum_{k\in K\setminus\{0\}} \hat{h}_{1,k}(J)e^{i\cdot k\cdot\phi},$$

the equation can be solved, provided the generating flow W_1 itself has the form:

$$W_1 = \sum_{k\in K\setminus\{0\}} w_{1,k}(J)e^{i\cdot k\cdot\phi},$$

leading to the solution

$$w_{1,k} = \frac{\hat{h}_{1,k}}{ik\cdot\omega}\quad \forall k\in K\setminus\{0\}, \tag{11}$$

where $k = (k_1,\ldots,k_d)$ and the last equation follows by implementing the Poisson brackets, calculating the derivatives and comparing coefficients of same Fourier order. The solution gives rise to small divisors of the form $k\cdot\omega = 0$, but since we are far away from resonances, we omit the introduction of the resonant module to exclude them in (11). The implementation of this transformation completes one iteration step of the Lie–transformation method. In a similar way, we may eliminate terms of second and higher order n in an algorithmic way described above and finally get the Hamiltonian in normal form:

$$H^{(n)}(J^{(n)},\phi^{(n)}) = Z^{(n)}(J^{(n)}) + R^{(n+1)}(J^{(n)},\phi^{(n)}),$$

where $Z^{(n)}$ and $R^{(n+1)}$ are called the normal form and remainder at order n, respectively. Fixing the order of normalization $n = n_{opt}$ and introducing the shorthand notation $'$ (prime) for new variables, the shifted frequencies of the system are given by

$$\omega'_k(J') = \frac{\partial Z^{(n_{opt})}}{\partial J_k'^{(n_{opt})}},$$

for $k = 1, \ldots, d$, while the higher order terms can be bounded by the norm of the remainder

$$O(J', \phi') \leq \left| \frac{\partial R^{(n_{opt}+1)}}{\partial \phi_k^{(n_{opt})}} \right|.$$

The last estimate will be used in order to find the stability time.

Let us apply the normal form algorithm to the approximate Hamiltonian of the Sitnikov problem given by Eqs. (8); we denote by k_j the non–zero average contribution of the term h_j computed in the new variables. Then, the normal form at order n can be written as $Z^{(n)} = \sum_{j=0}^{n} k_j$. We provide as an example the first terms up to the fourth order. We get

$$\begin{aligned} k_0 &= 2\sqrt{2}J_1 + J_2, \\ k_1 &= k_2 = k_3 = 0, \\ k_4 &= \frac{1}{4}\left(6\sqrt{2}e^2 J_1 - 9J_1^2\right). \end{aligned}$$

Higher orders can be constructed in a similar way, in order to obtain a normal form plus a remainder as

$$H\left(J_1, J_2, \phi_1, \phi_2; e\right) = Z^{(n)}\left(J_1, J_2; e\right) + R^{(n+1)}\left(J_1, J_2, \phi_1, \phi_2; e\right), \tag{12}$$

for some $n \in \mathbb{N}$.

4 Stability estimates in the Sitnikov problem

4.1 Some estimates of the remainder

In this section we provide estimates of the long term stability for given initial conditions by a detailed investigation of the remainder of the normal form. Due to the singularity of the action–angle variables near the origin, we introduce the set of non-singular Birkhoff Cartesian variables (see Fassò et al. 1998, Guzzo et al. 1998 for further details) as

$$w = \frac{v_z - iz}{i\sqrt{2}}, \quad u = \frac{v_z + iz}{\sqrt{2}},$$

which will transform a term of the series expansions of the form $ae^b {J_1}^c e^{-i(k_1\phi_1 + k_2\phi_2)}$ into terms of the form $a'e^b w^{c'} u^{d'} e^{-i(k_2\phi_2)}$. Here $a, a' \in \mathbb{C}$ are complex coefficients, $b, c, c', d' \in \mathbb{Z}_+$ are integer exponents and $k_1, k_2 \in \mathbb{Z}$ are integer numbers. The transformation can be done straightforward. We define the norm of a function $f = f(w, u, \phi_2)$ which is expanded in Birkhoff variables:

$$f = \sum_{m \in \mathbb{I}} a_m e^{b_m} w^{c_m} u^{d_m} e^{k_{2m}\phi_2}$$

as

$$\|f\|_{r,s} = \sum_{m \in \mathbb{I}} |a_m| \, e^{b_m} r^{c_m + d_m} e^{|k_{2m} s|},$$

where $\mathbb{I}$ is a finite index set to label the terms of the series expansion and r, s are the analyticity parameters. For the statement of the stability estimates we also need bounds of derivatives of a function $f = f(w(J_1, \phi_1), u(J_1, \phi_1), J_2, \phi_2)$ with respect to the angle ϕ_1. An easy calculation shows

$$\|\partial f\|_{r,s} \equiv \left\| \frac{\partial f}{\partial \phi_1} \right\|_{r,s} \le \left\| \frac{\partial f}{\partial w}\frac{\partial w}{\partial \phi_1} + \frac{\partial f}{\partial u}\frac{\partial u}{\partial \phi_1} \right\|_{r,s} \le C^{(0)} \left\| \left(\frac{\partial f}{\partial w} + \frac{\partial f}{\partial u} \right) \right\|_{r,s}$$

where the constant $C^{(0)}$ is given by

$$C^{(0)} = \left\| \frac{\partial w}{\partial \phi_1} \right\| + \left\| \frac{\partial u}{\partial \phi_1} \right\|,$$

and where we write ∂f for short.

We replace the new coordinates in the various series expansions given in the previous section; up to the fourth order, the approximate Hamiltonian is (up to machine precision):

$$\begin{aligned}
h_0 &= 2.82\, i\, uw + J_2, \\
h_1 &= h_2 = 0, \\
h_3 &= -1.68\, e \exp\{-i\phi_2\} u^2 - 1.68\, e \exp\{i\phi_2\} u^2 + 4.74\, i\, e \exp\{-i\phi_2\} uw \\
&\quad + 4.74\, i\, e \exp\{i\phi_2\} uw + 1.68\, e \exp\{-i\phi_2\} w^2 + 1.68\, e \exp\{i\phi_2\} w^2, \\
h_4 &= -1.68\, e^2 u^2 - 2.53\, e^2 \exp\{-2i\phi_2\} u^2 - 2.53\, e^2 \exp\{2i\phi_2\} u^2 - 0.66\, u^4 \\
&\quad + 4.74\, i\, e^2 uw + 7.11\, i\, e^2 \exp\{-2i\phi_2\} uw + 7.11\, i\, e^2 \exp\{2i\phi_2\} uw + 3.86\, i\, u^3 w \\
&\quad + 1.68\, e^2 w^2 + 2.53\, e^2 \exp\{-2i\phi_2\} w^2 + 2.53\, e^2 \exp\{2i\phi_2\} w^2 + 7.68\, u^2 w^2 \\
&\quad - 3.86\, i\, uw^3 - 0.66 w^4.
\end{aligned}$$

The normal form up to 4th order becomes:

$$\begin{aligned}
k_0 &= 2.82\, i\, uw + J_2, \\
k_1 &= k_2 = k_3 = 0, \\
k_4 &= 2.12\, i\, e^2 uw + 2.25\, u^2 w^2.
\end{aligned}$$

The generating function can be written as:

$$\begin{aligned}
w_0 &= w_1 = w_2 = 0, \\
w_3 &= -0.24\, i\, e \exp\{-i\phi_2\} u^2 - 0.13\, i\, e \exp\{i\phi_2\} u^2 + 2.03\, e \exp\{-i\phi_2\} uw \\
&\quad + 0.08\, e \exp\{i\phi_2\} uw - 0.13\, i\, e \exp\{-i\phi_2\} w^2 - 0.24\, i\, e \exp\{i\phi_2\} w^2, \\
w_4 &= -0.18\, i\, e^2 u^2 - 0.50\, i\, e^2 \exp\{-2i\phi_2\} u^2 - 0.14\, i\, e^2 \exp\{2i\phi_2\} u^2 \\
&\quad - 0.05\, i\, u^4 + 1.30\, e^2 \exp\{-2i\phi_2\} uw - 1.30\, e^2 \exp\{2i\phi_2\} uw \\
&\quad - 0.34\, u^3 w - 0.18\, i\, e^2 w^2 - 0.14\, i\, e^2 \exp\{-2i\phi_2\} w^2 - 0.50\, i\, e^2 \exp\{2i\phi_2\} w^2 \\
&\quad - 0.34\, uw^3 + 0.05\, i\, w^4.
\end{aligned}$$

The remainder of order 5 turns out to be:

$$
\begin{aligned}
r_5 = &-1.89\, e^3 \exp\{-i\phi_2\}u^2 - 1.89\, e^3 \exp\{i\phi_2\}u^2 - 3.72\, e^3 \exp\{-3i\phi_2\}u^2 \\
&-3.72\, e^3 \exp\{3i\phi_2\}u^2 - 1.65\, e \exp\{-i\phi_2\}u^4 - 1.65\, e \exp\{i\phi_2\}u^4 \\
&+5.33\, i\, e^3 \exp\{-i\phi_2\}uw + 5.33\, i\, e^3 \exp\{i\phi_2\}uw + 10.48\, i\, e^3 \exp\{-3i\phi_2\}uw \\
&+10.48\, i\, e^3 \exp\{3i\phi_2\}uw + 9.65\, i\, e \exp\{-i\phi_2\}u^3 w + 9.65\, i\, e \exp\{i\phi_2\}u^3 w \\
&+1.89\, e^3 \exp\{-i\phi_2\}w^2 + 1.89\, e^3 \exp\{i\phi_2\}w^2 + 3.72\, e^3 \exp\{-3i\phi_2\}w^2 \\
&+3.72\, e^3 \exp\{3i\phi_2\}w^2 + 19.21\, e \exp\{-i\phi_2\}u^2 w^2 + 19.21\, e \exp\{i\phi_2\}u^2 w^2 \\
&-9.65\, i\, e \exp\{-i\phi_2\}uw^3 - 9.65\, i\, e \exp\{i\phi_2\}uw^3 - 1.65\, e \exp\{-i\phi_2\}w^4 \\
&-1.65\, e \exp\{i\phi_2\}w^4.
\end{aligned}
$$

Using the same notation of the previous Section, we write up to the order n, respectively, the Hamiltonian, the normal form, the generating function and the remainder as

$$
H_n = \sum_{m=0}^{n} h_m, \quad Z_n = \sum_{m=0}^{n} k_m, \quad W_n = \sum_{m=0}^{n} w_m, \quad R^{(n+1)} = \sum_{m>n+1} r_m
$$

for short. We denote by $\| R^{(n+1)} \|_{r,s}$ the norm of the remainder and by $\| \partial W_n \|_{r,s}$ the norm of the derivative of the generating function as defined above.

First of all, we want to show the behavior of the norm of the remainder as function of the order of truncation n. We provide some examples in Figs. 3, 4 and 5 in order to analyze the global behavior of $\| R^{(n+1)} \|_{r_0,s}$ as e and r_0 vary, where r_0 is the parameter which defines the analyticity domain for the Cartesian coordinates (w, z) in the Hamiltonian normalized up to the zero order. The parameter s defines the analyticity domain for the angular variable ϕ_2 and it is fixed as $s_0 = 0.1$ in the following computations.

In Fig. 3a we provide $\| R^{(n+1)} \|_{r_0,s_0}$ versus n for fixed $e = 0.05$ and $r_0 = 0.05$ (marked by a filled disk in Fig. 4). In Fig. 3a the red (light) dots mark odd orders of normalization, blue dots (dark) mark even; for better visibility the dots are connected by lines. As one can see, the value of the norm of the remainder at $n_{opt} = 39$ is $\| R^{(40)} \|_{r_0,s_0} \simeq 0.6 \times 10^{-11}$ (which corresponds to the filled disk in Fig. 5). In Fig. 3b we provide the norm of the remainder series for $e = 0.15$ and $r_0 = 0.15$ versus the normalization order (filled diamond in Figs. 4, 5). The optimal order of truncation turns out to be 30 and the norm of the remainder $\| R^{(31)} \|_{r_0,s_0} \simeq 0.5 \times 10^{-2}$ (see also diamond in Fig. 5). The case $n_{opt} = 5$ is shown in Fig. 3c with $\| R^{(6)} \|_{r_0,s_0} \propto 0.5 \times 10^{-1}$. We mark the example with a filled square in Figs. 4 and 5. In Fig. 4 we plot the optimal order of truncation $n = n_{opt}$ obtained by minimizing $\| R^{(n+1)} \|_{r_0,s_0}$ with respect to the normalization order n in the parameter space (r_0, e). Within the contour–line $n_{opt} = 35$ the optimal order of truncation is not reached within the normalization order 39 while outside the contour–line with optimal order of truncation 10, the optimal order n_{opt} is already reached below or at order 5. The range $n_{opt} \in \{10, 35\}$ lies close to an arc starting at around $(e, r_0) = (0, 0.3)$ and ending at around $(e, r_0) = (0.23, 0)$. The plot of Fig. 5 shows the exponent j of the norm of the remainder $\| R^{(n+1)} \|_{r_0,s_0} \propto 10^{-j}$ at the optimal order of truncation n_{opt} in the parameter space (r_0, e). The contour–line $\| R^{(n+1)} \|_{r_0,s_0} \propto 0.1$ lies close to the boundary of the optimal order of truncation $n_{opt} > 5$ of Fig. 4 but extends to larger values in e as r_0 increases. The stability time (related to the inverse of the norm of the remainder) increases by decreasing parameters r_0 and e.

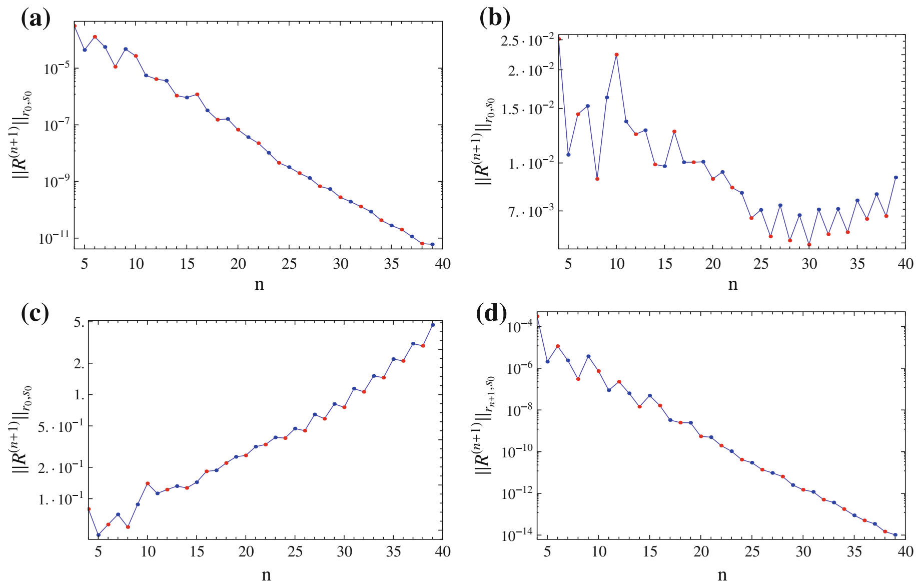

Fig. 3 The first three plots show the norm of the remainder $\|R^{(n+1)}\|_{r_0,s_0}$ as function of the normalization order n for fixed $s_0 = 0.1$ and for different values of r_0 and e. **a** $r_0 = 0.05$, $e = 0.05$ (*filled disk* in Figs. 4, 5); the norm is a decreasing function of the order n and its minimum is reached at order 39. **b** $r_0 = 0.15$, $e = 0.15$ (*dark diamond* in Figs. 4, 5); the minimum is reached at order 30. **c** $r_0 = 0.2$, $e = 0.2$ (*filled square* in Figs. 4, 5); the norm is an increasing function of the order n and the minimum is reached at order 5. **d** The last plot shows the norm of the remainder $\|R^{(n+1)}\|_{r_{n+1},s_0}$ versus the normalization order n for $r_0 = 0.05$, $e = 0.05$ and for $s_0 = 0.1$. Note that the norm is now computed at each step for the corresponding r_n, while in Figures a,b,c the norm is computed at each step for a fixed r_0. For $n = n_{opt} = 39$ we get $r_{40} = 0.015$ with $\|R^{(40)}\|_{r_{40},s_0} \simeq 0.1 \times 10^{-13}$ (the point $(e, r_n) = (0.05, 0.015)$ is marked by a *red star* in Figs. 4, 5)

For the statement of the stability results we also need to take into account the change of the analyticity domain in r versus the normalization order n. Starting from r_0 which bounds the analyticity domain of the normalized Hamiltonian up to the zero order, we know that the domain of the normalized Hamiltonian up to the order n can be bound by using the deformation of the new variables obtained by means of the generating function:

$$\|r_{n+1} - r_n\| \leq \|\partial W_n\|_{r_n,s_0}.$$

In Fig. 6a, b we plot r_n versus normalization order n for different values of e and r_0, respectively. If the parameter r_0 and e are smaller than critical values, the decrease of r_n is largest at the first normalization steps and becomes smaller and smaller with the ongoing normalization. The situation changes if the parameters become too large, namely, the norm of the derivative of the generating function increases too much with increasing normalization order. In that case we loose the analyticity domain before we reach the optimal order of truncation (it means that r_n goes to 0 for $n < n_{opt}$). We label the domain where we can exclude this behavior by a dashed rectangle in Figs. 4, 5. The loss of the analyticity domain in r_n for the parameter $e = 0.05$ and $r_0 = 0.05$ (filled disk) is indicated by a dashed line ending in $e = 0.05$ and $r_n = 0.015$ (marked with a red star). In Fig. 3a, the norm of the remainder is computed for fixed value of r_0 for each n. In Fig. 3d, we plot again the norm of the remainder series $\|R^{(n+1)}\|_{r_{n+1},s_0}$ versus the normalization order n in which the norm is computed for the corresponding r_n at each order n. Compared to the plot shown in Fig. 3a the norm of the

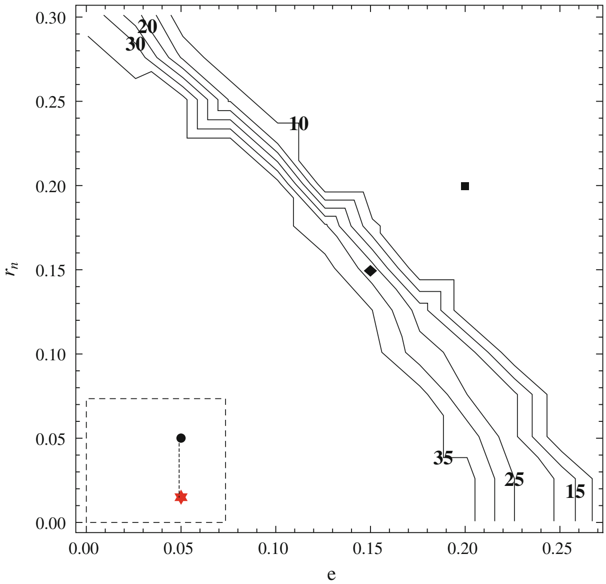

Fig. 4 The figure shows the optimal order of truncation r_{opt} (given by the *numbers* inside the plot) of the norm $\|R^{(n+1)}\|_{r_0,s_0}$ in the parameter space $r_0 \times e$ for $s_0 = 0.1$. Within the contour–line $r_{opt} = 35$ the optimal order of truncation is not reached within the normalization order 39 while, outside the contour–line with optimal order of truncation 10, the optimal order r_{opt} is already reached below or at order 5. The range $r_{opt} \in \{10, 35\}$ forms an arc starting at around $(e, r_0) = (0, 0.3)$ and ending at around $(e, r_0) = (0.23, 0)$. The corresponding plots of the remainder series versus normalization order for the rectangle, the disk, the diamond and the star are shown in Fig. 3a, b, c, d, respectively. The *dashed rectangle marks* the region where for given r_0 the domain of analyticity does not vanish after the normalization: in fact, we have $r_{40} > 0$ at normalization order 39. The *dashed line* connecting the filled disk and the red star indicates the loss of analyticity domain in terms of r_n as $n = 39$ (compare with Fig. 6b)

remainder at the optimal order of truncation becomes $\|R^{(40)}\|_{r_{40},s_0} \simeq 0.1 \times 10^{-13}$ (see also Fig. 5).

4.2 Stability estimates of the solution

The distance between the solution at time $t > 0$ and the initial condition can be bounded as (see, for example, Pöschel 1993):

$$\|J(t) - J(0)\| \leq \|J(t) - J^{(n)}(t)\| + \|J^{(n)}(t) - J^{(n)}(0)\| + \|J^{(n)}(0) - J(0)\|$$

where $J^{(n)} = i w^{(n)} u^{(n)}$ is the radial distance from the central equilibrium point; $w^{(n)}$, $u^{(n)}$ are the Birkhoff variables at normalization order n and $J \equiv J^{(0)}$ is the distance in terms of the original variables. The effect of the transformation can be bounded by

$$\|J(t) - J^{(n)}(t)\| < C_{\rho,e}{}^{(1)}\varepsilon, \quad \|J^{(n)}(0) - J(0)\| < C_{\rho,e}{}^{(1)}\varepsilon,$$

where ρ is the fixed parameter labeling the original distance from the equilibrium, $C_{\rho,e}{}^{(1)}$ is a constant related to the norm of the generating function via $\|\partial W_n\|_{\rho,s_0} \leq C_{\rho,e}{}^{(1)}\varepsilon$ and $\varepsilon = \max(\rho, e)$ is the largest of the two small parameters ρ and e. Furthermore we bound the effect of the remainder on the dynamics by the trivial estimate:

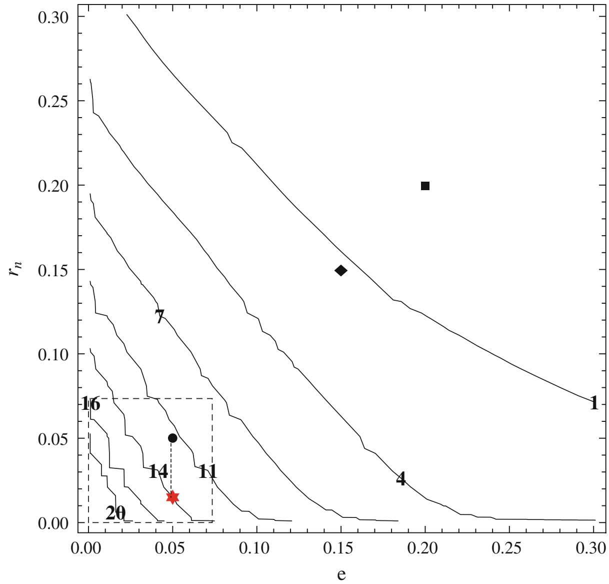

Fig. 5 The plot shows the exponent j of the norm of the remainder $\|R^{(n+1)}\|_{r_0,s_0} \propto 10^{-j}$ at the optimal order of truncation $n = n_{opt}$ in the parameter space $r_0 \times e$. The contour–line $\|R^{(n+1)}\|_{r_0,s_0} \propto 0.1$ lies close to the boundary of the optimal order of truncation $n_{opt} > 5$ of Fig. 4 but extends to larger values in e as r_0 increases. The stability time (related to the inverse of the norm of the remainder) increases with decreasing parameters r_0 and e. The *dashed rectangle marks* the region where for given r_0 the domain of analyticity does not vanish at normalization order $n = 39$. The corresponding plots of the remainder series versus normalization order for the *square*, *the disk*, *the diamond* and *the star* are shown in Fig. 3a, b,c,d, respectively

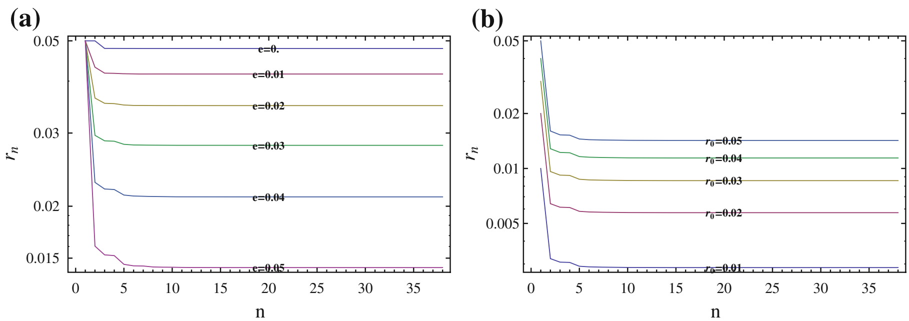

Fig. 6 The figures show r_n versus normalization order n; the plot (**a**) is obtained for fixed initial $r_0 = 0.05$ and different values of $e \in (0, 0.05)$. The plot (**b**) is obtained for fixed value of $e = 0.05$ and for different initial $r_0 \in (0.01, 0.05)$. In both cases, by increasing the normalization order n, r_n tends to a constant value

$$\|J^{(n)}(t) - J^{(n)}(0)\| \leq \int_0^t \left\| \frac{\partial R^{(n+1)}}{\partial \phi_1} \right\|_{\rho,s_0} dt \leq \int_0^t \|\partial R^{(n+1)}\|_{\rho,s_0} dt \leq t C_{\rho,e}{}^{(2)} \varepsilon^{n+1}$$

where $C_{\rho,e}{}^{(2)}$ is related to the norm of the remainder via $\|\partial R^{(n+1)}\|_{\rho,s_0} < C_{\rho,e}{}^{(2)} \varepsilon^{n+1}$. By setting $t C_{\rho,e}{}^{(2)} \varepsilon^{n+1} < C_{\rho,e}{}^{(1)} \varepsilon$ and the choice of n such that $\varepsilon^{-n} = T_0 e^{1/\varepsilon}$ we get

Table 1 Stability results and constants along the line $e = 0.05$, $r_0 \leq 0.05$ and along the line $r_0 = 0.05$, $e \leq 0.05$ (dashed rectangle in Figs. 4, 5) given by formulas of Sect. 4.2

r_0	e	r_{40}	$C^{(1)}_{\rho,e}$	$C^{(2)}_{\rho,e}$	T_0	R_0	T	ΔJ
0.01	0.05	0.0028	0.158	1.65×10^{36}	109000	0.475	5.28×10^{13}	0.0238
0.02	0.05	0.0057	0.320	6.91×10^{36}	52500	0.960	2.54×10^{13}	0.048
0.03	0.05	0.0085	0.488	1.68×10^{37}	32900	1.46	1.60×10^{13}	0.0732
0.04	0.05	0.0114	0.665	3.33×10^{37}	22700	2.	1.10×10^{13}	0.0998
0.05	0.05	0.0142	0.856	5.97×10^{37}	16200	2.57	7.88×10^{12}	0.128
0.05	0.01	0.0416	0.185	1.74×10^{33}	1.2×10^{8}	0.555	5.83×10^{16}	0.0277
0.05	0.02	0.0349	0.337	1.10×10^{35}	3.47×10^{6}	1.01	1.69×10^{15}	0.0505
0.05	0.03	0.0280	0.498	1.42×10^{36}	396000	1.49	1.92×10^{14}	0.0747
0.05	0.04	0.0211	0.67	1.09×10^{37}	69700	2.01	3.38×10^{13}	0.101
0.05	0.05	0.0142	0.856	5.97×10^{37}	16200	2.57	7.88×10^{12}	0.128

$$t \leq \frac{{C_{\rho,e}}^{(1)}}{{C_{\rho,e}}^{(2)}} \varepsilon^{-n} \leq T_0 \exp\left\{\frac{1}{\varepsilon}\right\}$$

for some T_0 with ${C_{\rho,e}}^{(1)}/{C_{\rho,e}}^{(2)} < T_0$. Writing $R_0 = 3{C_{\rho,e}}^{(1)}$ the stability statement finally becomes

$$\Delta\mathrm{J} \equiv \|J(t) - J(0)\| \leq R_0\varepsilon \quad \text{for any} \quad t < T \equiv T_0 e^{\frac{1}{\varepsilon}}.$$

A careful evaluation of the constants can be done for given parameters r_0 and e. For example, for $r_0 = 0.05$, $e = 0.05$ (filled disk in Figs. 4, 5) and by setting $\varepsilon = 0.05$, we find $R_0 = 2.57$, $T_0 = 16200$, and the bound of the variation in action space turns out to be about $\Delta\mathrm{J} = 0.13$ for $T = 7.88 \times 10^{12}$. In Table 1 we provide stability results for different values of r_0 and e (taken in the dashed rectangle in Figs. 4, 5).

5 Summary and conclusions

In the present paper we derive for the first time locally valid exponential stability estimates for the motion of the massless body in the Sitnikov problem. The estimates are based on the proper construction of a non–resonant normal form of the approximate Hamiltonian flow, which describes the motion close to the central equilibrium of the system. The results are valid for moderate values of the eccentricity of the primary bodies and for small oscillations of the third body only.

The methodology to obtain our results is the following: we derive the approximate Hamiltonian model as well the locally valid equations of motion in terms of expansion series around $e = 0$ and $z = 0$. Then we provide the method to construct the normal form based on Lie–series and give the explicit normal form Hamiltonian to low orders. To obtain the estimates we also construct the remainder of the normal form to high orders (40) by computing the necessary series expansions numerically.

The stability estimates are derived from the norm of the generating function and the norm of the remainder series given in action–angle variables. It is known that the use of action–angle variables of the harmonic oscillator does not allow to analyze the problem near the periodic orbit, due to the known singularity of the actions at the equilibrium solution. For this reason we obtain the various series expansions in terms of Birkhoff coordinates. We find the transformation and provide the formulae, numerically to low orders.

We study the dependence on the parameters involved in the problem, namely the eccentricity e and the distance r from the elliptic equilibrium. We find numerically the optimal order of truncation in the parameter space $e \times r$, namely the order of truncation such that the remainder is minimal and we use the norm of the remainder in order to give stability estimates. The evolution of the action variables of the original problem is estimated through the norm of the remainder and the norm of the generating function in a suitable domain of the space $e \times r$.

The task to obtain exponential stability estimates in the Sitnikov problem is not a trivial one. On the one hand the estimates cannot directly be derived in terms of action–angle variables due to the singularity of them close to the central equilibrium. On the other hand no proper Nekhoroshev–like statement without making use of action–angle like variables exists for non isochronous systems. In the present approach the problem to obtain the estimates could be solved by the implementation of a high order normal form and by using the remainder of it in order to find the exponential stability estimates. It can be seen as a first step for the development of a theory of Nekhoroshev–like estimates for non isochronous dynamical problems without making use of action–angle variables.

Acknowledgments We thank A. Celletti for many ideas, U. Locatelli, A. Giorgilli for fruitful discussions and C. Efthymiopoulos for providing us with the Fortran programs. A special acknowledgement is for M. Guzzo for an excellent review of the paper. This project is partly supported by the grants *ASI, "Studi di Esplorazione del Sistema Solare"* and the PRIN 2007B3RBEY "Dynamical Systems and applications" of MIUR.

References

Belbruno, E., Libre, J., Ollé, M.: On the families of periodic orbits which bifurcate from the circular Sitnikov motions. Celest. Mech. Dyn. Astron. **60**, 99–129 (1994)

Bountis, T., Papadakis, K.E.: The stability of vertical motion in the N–body circular Sitnikov problem. Celest. Mech. Dyn. Astron. **104**, 205–225 (2009)

Dvorak, R.: Numerical results to the Sitnikov problem. Celest. Mech. Dyn. Astron. **56**, 71–80 (1993)

Dvorak, R., Sun, Y.S.: The phase space structure of the extended Sitnikov problem. Celest. Mech. Dyn. Astron. **67**, 87–106 (1997)

Efthymiopoulos, C.: On the connection between the Nekhoroshev theorem and Arnold diffusion. Celest. Mech. Dyn. Astron. **102**, 49–68 (2008)

Faruque, S.B.: Solution of the Sitnikov problem. Celest. Mech. Dyn. Astron. **87**, 353–369 (2003)

Fassò, F., Guzzo, M., Benettin, G.: Nekhoroshev–stability of elliptic equilibria of Hamiltonian systems. Commun. Math. Phys. **197**, 347–360 (1998)

Ferraz–Mello, S.: Canonical Theories of Perturbation, Degenerate Systems and Resonance. Springer, New York (2006)

Giorgilli, A.: Notes on exponential stability of Hamiltonian systems. In: Dynamical Systems. Part I: Hamiltonian Systems and Celestial Mechanics, Pubblicazioni della Classe di Scienze, Scuola Normale Superiore, Pisa. Centro di Ricerca Matematica "Ennio De Giorgi": Proceedings; Scuola Normale Superiore, Pisa (2002)

Guzzo, M., Fassò, F., Benettin, G.: On the stability of elliptic equilibria. Math. Phys. Electron. J. **4**, 1 (1998)

Hagel, J.: An analytical approach to small amplitude solutions of the extended nearly circular Sitnikov problem. Celest. Mech. Dyn. Astron. **103**, 251–266 (2009)

Hagel, J.: A new analytic approach to the Sitnikov Problem. Celest. Mech. Dyn. Astron. **53**, 267–292 (1992)

Hagel, J., Lhotka, C.: A high order perturbation analysis of the Sitnikov Problem. Celest. Mech. Dyn. Astron. **93**, 201–228 (2005)

Hagel, J., Trenkler, T.: A computer aided analysis of the Sitnikov problem. Celest. Mech. Dyn. Astron. **56**, 81–98 (1993)

Kovács, T., Érdi, B.: Transient chaos in the Sitnikov problem. Celest. Mech. Dyn. Astron. **105**, 289–304 (2009)
Liu, J., Sun, Y.S.: On the Sitnikov problem. Celest. Mech. Dyn. Astron. **49**, 285–302 (1990)
MacMillan, W.D.: An integrable case in the restricted problem of three bodies. Astron. J. **27**, 11–13 (1913)
Moser, J.: Stable and Random Motions in Dynamical Systems. Princeton University Press, Princeton (1973)
Nekhoroshev, N.: An exponential estimate of the time of stability of nearly integrable Hamiltonian systems. Russ. Math. Surv. **32**, 1–65 (1977)
Pöschel, J.: Nekhoroshev estimates for quasi–convex Hamiltonian systems. Math. Z. **213**, 187–216 (1993)
Sidorenko, V.V.: On the circular Sitnikov problem: the alternation of stability and instability in the family of vertical motions. Celest. Mech. Dyn. Astron. **109**, 367–384 (2011)
Sitnikov, K.A.: Existence of oscillatory motion for the three–body problem. Dokl. Akad. Nauk. USSR **133**(2), 303–306 (1960)
Soulis, P., Bountis, T., Dvorak, R.: Stability of motion in the Sitnikov 3–body problem. Celest. Mech. Dyn. Astron. **99**(2), 129–148 (2007)
Stumpff, K.: Himmelsmechanik I. VEB, Deutscher Verlag der Wissenschaften, Berlin (1959)